

Mechanical Reliability of Devices Subdermally Implanted into the Young of Long-Lived and Endangered Wildlife

Bryan Hori, Royann J. Petrell, Goran Fernlund, and Andrew Trites

(Submitted March 5, 2010)

Service data does not exist for the strength of enclosures for subdermally implanted biotelemetry devices intended for young wild animals. Developing adequate tests especially for implants intended for endangered species is difficult due to the very limited availability of live animals and cadaverous tissue, ethical concerns about using them, and high enclosure costs. In this research, these limitations were overcome by taking a conservative approach to design and testing. Reliability tests were developed and performed to establish the likelihood that a thin subdermally and cranially implanted alumina enclosure would fail due to typical external forces related to diving, fights, and falls over the expected 30-year life time of sea lions. Cyclic fatigue tests indicative of deep dives performed out of tissue and at the 90% reliability level indicated no failure after 70,000 stress cycles at stresses of approximately 15 MPa; dynamic fatigue tests indicated a 5% probability of failure at 250 MPa; and puncture tests indicative of fight bites showed a 5% probability of failure at 1500 N. These values were far outside of what the animals might expect to encounter in real life. On the other hand, the response of the enclosure to impact outside of the tissue was failure at a mean energy level of 6.7 J. Modeling results predict that head impacts due to trampling by fighting sea lion males and falls over 1 m onto a rocky ledge typical of haul out environments would likely fracture an infant's head as well as the implant. The device can be implanted under an impact absorbing 1 cm blubber layer for extra protection. More service data for enclosures can be made more available despite limited availability of test animals if a conservative approach to testing is taken.

Keywords alumina, biomaterials, biotelemetry, mechanical testing, Sea Lion, structural ceramics

1. Introduction

Wildlife implantable telemetry devices, unlike human implants, generally cannot be removed if defective or at end of service life. Instead, they are left inside the animal. For long-living animals such as marine mammals, implantation periods can range between 20 and 100 years depending on the species (Ref 1). Another difference between wildlife and human implants is the availability of reliability data, which help to identify any problems with usage. In wildlife telemetry implants, reliability is generally restricted to electronic function. Data showing how an implant enclosure withstands exterior, interior (e.g., battery corrosive), and cellular modes of degradation are limited. The lack of enclosure service data is particularly alarming when the implant is intended for the most vulnerable, or very young and endangered species. The lack of reliability data also makes it difficult to plan and execute research intended for the protection of wildlife.

Bryan Hori and Royann J. Petrell, Chemical and Biological Engineering, The University of British Columbia, 2360 East Mall, Vancouver, BC V6T 1Z3, Canada; Goran Fernlund, Materials Engineering, The University of British Columbia, 6350 Stores Road, Vancouver, BC V6T 1Z4, Canada; and Andrew Trites, UBC Marine Mammal Research Unit, Rm 247 AERL, 2202 Main Mall, Vancouver, BC V6T 1Z4, Canada. Contact e-mail: rpetrell@chbe.ubc.ca.

In this research, the mechanical reliability of a thin enclosure for a biotelemetry device intended for implantation under the cranial skin behind the occipital crest of a Steller sea lion pup (life expectancy >20 years) was assessed (Fig. 1a). The Steller sea lion is endangered over much of its range (Ref 2). The top of the head was chosen for the implant location because it is expected to be the most protected against impact and occlusion by other animals and well suited for signal propagation. Young animals have little muscle and skin tissues there, and this and the thinness of the device make implant surgery less invasive and the implant less affected by muscle contraction (Ref 3). The near absence of soft tissue between the implant site and the skin in pups means, however, that there would be little tissue to dampen the effects of exteriorly applied forces. Testing data were used to determine the likelihood that the enclosure would not fail mechanically, and therefore, protect the animal over its lifetime. Issues relating to biocompatibility have been reported elsewhere (Ref 3).

Tests that are used to predict service performance must reflect actual loading conditions and intended service life. For example, hip implants are designed to last up to 40 years, and endure many types of loadings. Accelerated testing methods have been developed to simulate 40 years of service time of hip implants in 6 months (Ref 4). However, testing costs and time constraints generally limit the number and type of tests actually performed. The availability of endangered animals and their tissues is also extremely limited. Loading conditions in this study were selected based on expected loading conditions, such as pressures due to deep sea diving, puncture forces due to fighting, and impact dynamic forces due to falls or collisions with other animals. It is expected that this research will promote the testing of implant enclosures for other forms of wildlife and service conditions.

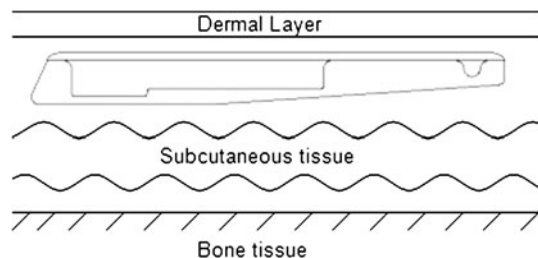


Fig. 3 In-service placement of implanted enclosure

of the test set-up leads to conservative experiments as in practice the enclosure sits on top of soft tissue and bone (Fig. 3).

The expected pressures were determined from available dive records of depth, dive duration, and dive frequency from 25 Steller sea lion pups (Ref 6). The mean dive depth was 135 m with a mean dive frequency of approximately 6.3 times a day. The mean pressure associated with this dive is 1.33 MPa, and the total number of cycles for a Steller sea lion living a lifespan of 30 years is 68 985 cycles (Ref 7). Thus, the enclosure needs to sustain at least a mean fatigue stress of 1.33 MPa for 68 985 cycles. To account for strength degradations resulting from tissue growth after implantation, maximum and minimum stresses of 14.95 and 0.57 MPa, respectively, were selected (mean stress 7.76 MPa), and enclosure samples were cycled with a sinusoidal compressive stress profile for 70,000 times. Ten sample enclosures were tested, and a binomial statistical test method used for small sample sizes was used to characterize the acceptability of the housing to the specified test conditions by classifying test trials as successes or failures (Ref 8)

$$\sum_{x=0}^r \binom{r}{x} R^{n-x} (1-R)^x \leq 1 - C$$

with $R^n \leq 1 - C$ for the case of no failures (Eq 1)

A successful trial was when the enclosure did not fail before 70,000 cycles was reached. The low sample size (restricted due to funds and enclosure costs) leads to a low reliability at a high confidence level (90%) or a high reliability (90%) with low confidence level. The frequency of cyclic loading was 10 Hz. This frequency differed from actual loading conditions (Ref 6) so that the testing could be completed within a reasonable time. It has been reported that the effect of cycle frequency is negligible up to 20 Hz (Ref 9), 100 Hz (Ref 10), and 170 Hz (Ref 11) after which temperature effects may start to affect the results.

In addition to the cyclic compressive testing, quasi-static compressive strength testing was conducted using six enclosures to determine the maximum diving depth before the enclosure ruptures due to compression (i.e., maximum pressure the enclosure can withstand). Depths of over 400 m have been reported for Steller sea lion dives resulting in pressures over 4 MPa. The loading rate was the speed at which a Steller sea lion dives or 6.79 m/s (70 kPa/s) (Ref 6). The test set-up for the compressive strength tests included a Forney FX600 compression machine (Forney Inc., Forney, TX, USA). Results from the compressive strength tests were analyzed by constructing a Weibull diagram (Ref 12, 13), and the failure mode was recorded. Using this methodology, the failure probability, P , is related to the strength measurements using the following relationship:

$$P = 1 - \exp \left[- \left(\frac{\sigma}{\sigma_0} \right)^{m_w} \right], \quad (\text{Eq 2})$$

where m_w is the Weibull modulus, σ is the applied compressive strength, and σ_0 is a characteristic strength. By taking the double-logarithm of both sides of Eq 2

$$\ln \left[\ln \frac{1}{1-P} \right] = m_w \ln \left(\frac{\sigma}{\sigma_0} \right) \quad (\text{Eq 3})$$

The strength measurements were plotted on a graph, which allowed the determination of the Weibull modulus (slope) and the characteristic strength (from the intercept with the ordinate). The probability of failure P was calculated by ranking the failure tests, $i = 1, \dots, N$ (N = total number of tests), and using the following approximate formula for the probability of failure P at the i th strength level:

$$P(i) = \frac{i - 0.3}{N + 0.4} \quad (\text{Eq 4})$$

2.2.2 Puncture Forces as a Result of Steller Sea Lion Bites.

The fighting behavior of many seals and sea lions have been observed, and biting is the main conduit for harming each other. The possibility of the implant being bitten in an area subject to biting may be rare, but if it occurs it is important that the enclosure failure does not affect the wounded animal. The test apparatus for the cyclic pressure and puncture tests included a shield, pressure plate, enclosure holder as described previously in addition to a puncture head (Fig. 2b). The puncture head area represents the tip of mature Steller sea lion teeth (as determined by direct measurements on Steller sea lion skulls housed at the University of British Columbia).

Tests were conducted in air at room temperature. The variation in temperature that the enclosure could experience (approximately 5-10 °C) that would contribute to the mechanical response is negligible (Ref 14). Loading rate was that of the bite force rate for a human (i.e., 300 N/s), as rates for sea lions are not available (Ref 15). Loads were applied until failure of the enclosure. The failure load was recorded as a load versus time curve, and a load frame (Instron, Inc., Burlington, ON, Canada) under displacement control was used to apply the puncture loads. A Weibull probability diagram was again constructed to analyze the results.

The expected puncture force from a Steller sea lion is unknown, but as it is a predator, it can be assumed to lie somewhere due to its size close to that of an African lion or 1768 N (Ref 16). Flat or blunt teeth can exert much higher forces than pointed teeth since high stresses accumulate in pointed teeth at high loads, which could lead to tooth fracture. The force ratio is 4:2:1 for molars, premolars, and incisors, respectively (Ref 17). The highest forces occur when biting on hard surfaces. Steller sea lion teeth are pointed so the maximum force that the enclosure should be able to withstand is approximately 440 N.

Another concern is breaking the teeth of the biting animal when the animal bites down on the hard alumina surface. As the fracture load is not known for Steller sea lion teeth, twice the fracture loads for human teeth (800-1800 N) was assumed for the max breaking strength (Ref 18).

2.2.3 Impact Dynamic Forces from Falling or Interactions with Other Steller Sea Lions.

Impact forces vary depending on momentum, material properties, the area of impact and the type of surfaces in contact with the implant upon loading. Two worst case scenarios for the enclosures were

considered, namely (1) an animal free falling onto a hard smooth surface and (2) a pup being trampled by a large male (bull). The first scenario is associated both with the tendency of infants of large species to fall in general and the environmental habitat or the haul outs and rookeries (where pups are born and remain for approximately 3-4 months). Small rocky islands are often used as haul outs and rookeries, and they consist of many small cliffs where the animals rest (maximum height of 5 m). The first worst-case scenario occurs when a pup (approximately 23 kg at birth) falls off one of these cliffs to hit its head in the area of the implant against a rock. When young mammals fall, they have the tendency to fall in a headfirst orientation because of a lack of co-ordination and their disproportionately large heads as compared to adults (Ref 19, 20). The second scenario involves interactions with other sea lions especially large males (Ref 21, 22). Often there are territorial fights during the breeding period, and occasionally during these fights a pup gets trampled by a bull (200-1000 kg) (Ref 23). Subcutaneous implants can become damaged or displaced due to injuries from fighting and wound licking, as shown in surgical implantation of telemetry transmitters in European Badgers (Ref 24).

The approach to impact was two-fold. First, the impact strength was determined experimentally, and then, theoretical considerations were used to determine if the implant enclosure would break under the above-mentioned conditions before the skull would break. If the enclosure proved to be as strong as or stronger than the skull, then it was deemed to provide adequate protection.

To evaluate the mechanical reliability of the alumina enclosure under impact loads, drop-weight impact testers and pendulums are usually used (Ref 25-27). Drop tests were carried out at room temperature using a drop-weight impact tester using the Bruceton Staircase Method (Ref 28). For 11 samples, the height at failure for each sample was recorded. The test apparatus was built following ASTM standards (Ref 28, 29), and a mass of 4.89 kg was dropped onto samples. A starting point that corresponds to energies between 1 and 22 J was used because the fracture energy for the alumina falls within this range (Ref 30, 31). The first specimen was tested at a height of 130 mm corresponding to 6 J. If the specimen did not fracture, the height of the dropped weight was increased by 10 mm otherwise the height was reduced by 10 mm. Failure and non-failures are recorded and the mean failure height and energy are calculated as in Ref 28.

A failure criterion for a free fall was developed by calculating the kinetic energy at different fall heights. It was assumed that the acceleration was only due to gravity, g , and the fall occurs in a straight line a distance, S , without being impeded by drag from the initial fall position toward the point of impact. Velocity, V , at impact is, then, given by

$$V = \sqrt{2gS} \quad (\text{Eq 5})$$

and kinetic energy, K_c (J) of a pup of mass 23 kg by

$$K_c = 0.5 MV^2, \quad (\text{Eq 6})$$

where M is the head mass of a pup (0.25 of the total mass). The calculated energy is a conservative value as it assumes that the sea lion head falls directly on the implant with all kinetic energy being used converted to strain energy in the enclosure. In reality, surrounding tissues would absorb some of the kinetic energy in the same way ductile backings do when alumina is subjected to ballistic impact. Alumina is

used for its high strength, and a more ductile backing is often used to absorb the kinetic energy (which can exceed 1 kJ) (Ref 32-35). The impact energy human skulls have been reported to absorb without failing, ranges from 17 to 28 J (Ref 36, 37).

The second scenario is head and enclosure impact due to a trampling bull. To calculate the impact energy due to running, the general impulse equation ($F = m \cdot dV/dt$), and empirically derived ground foot contact time, t_c , and peak force, F , measures as a function of animal mass, M , were used (Ref 38). First, the velocity of impact due to running, V_r , was calculated

$$V_r = \frac{Ft_c}{0.25M_b} \quad (\text{Eq 7})$$

given values of F and t_c . The 0.25 in the above equation is due to the assumption that only a quarter of a bull mass, M_b , bears down on a foot (flipper) during running. For a 1000 kg bull, $t_c = 0.21$ s, $F = 24,500$ N, and $V_r = 20$ m/s. Kinetic energy of running was then calculated using V_r and M_b , and compared to impact energies for skulls and the alumina enclosure.

3. Experimental Results

3.1 Compressive Strength Tests—Static and Cyclic

The results are shown numerically in Table 1 and as a Weibull diagram (Fig. 4). A straight line fit to the data gave a characteristic strength of 553 MPa and a Weibull modulus of 3.92 ($R^2 = 0.92$). With the Weibull parameters determined, Eq 2 was used to plot the probability of failure as a function of the applied stress. Figure 5 shows that at an applied stress of 259 MPa, the probability of failure is <5%. 259 MPa is more than 60 times higher than the pressure seen at a maximum

Table 1 Failure forces and stresses from compression tests on six specimens

Specimen #	Force, kN	Stress, MPa
1	840.1	482.8
2	1060.5	609.5
3	538.5	309.5
4	1117.6	642.3
5	925.1	531.7
6	837.1	481.1

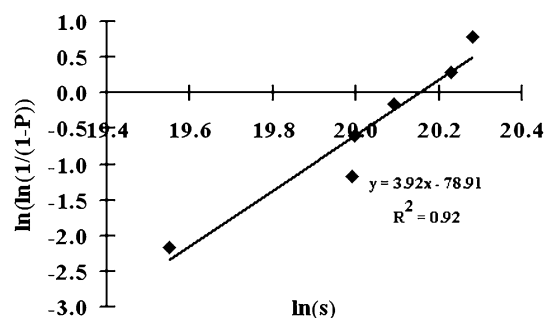


Fig. 4 Weibull diagram for compression tests

diving depth of 400 m. The measured strength is equivalent to failure at depths of 24,000 m; depths that far exceed the maximum capabilities of sea lions. Consistent with having most of the stress applied onto the side-walls, failure occurred in all enclosures with cracks in the interior of the enclosure wall.

In the cyclic compressive fatigue tests, all samples passed the tests using sinusoidally varying applied compressive stresses of 0.57-14.94 MPa for 70,000 cycles. Using the binomial statistical test method for no failures, these results correspond to a reliability of 90% with a 65% confidence level or a confidence level of 90% with 79% reliability for 10 samples. Using the binomial test method, a high reliability and confidence level means that it is likely the component will pass the test whenever subjected to the same loading condition.

3.2 Puncture Tests

Load-time diagrams were recorded for each of the six puncture tests. The bite of an animal can be considered a type of Hertzian contact load (as the tooth is rounded at the end) and thus, it is expected to generate similar types of cone cracking failure. Despite variations between tests, the load-time diagrams for the puncture experiments show several important features. The first characteristic is the point at which initial cracks begin to form. On the load-time plot, this corresponds to a drop-off in force that occurred at around 7 s for all samples. The maximum force that the enclosures could withstand was significantly higher (Table 2). A Weibull analysis of the load at first crack for the six samples gave a characteristic strength of 2015 N and a Weibull modulus of 11.83 ($R^2 = 0.97$), Fig. 6 and 7. At an applied puncture force of 1568 N, Fig. 7 gives the probability of failure $<5\%$.

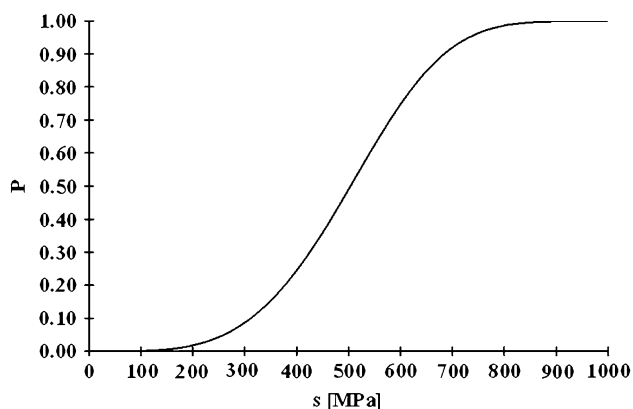


Fig. 5 Probability of failure of the enclosure vs. the applied compression stress

Table 2 Failure forces, first crack and maximum, from puncture tests on six specimens

Specimen #	Force—first crack, N	Force—maximum, N
1	2006.1	N/A
2	2065.2	6265.3
3	2118.9	6326.2
4	1686.6	6852.5
5	1966.9	5811.2
6	1792.5	5355.8

3.3 Impact Tests

Drop-weight impact tests were conducted on 11 specimens, and the results are summarized in Table 3. The mean failure height (using a 4.89 kg mass) was calculated to be 140 ± 69 mm with associated mean failure energy of 6.7 J. Of the 11 enclosures tested, 4 fractured. The observed fracture was localized and catastrophic failure of the enclosure did not occur. In all the four fractures, only chipping was observed as no discernable cracks could be seen which is in agreement with observations for impact failure reported in the literature (Ref 39).

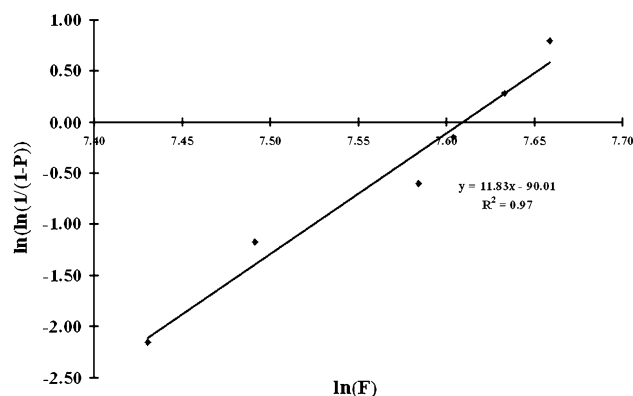


Fig. 6 Weibull diagram for puncture tests

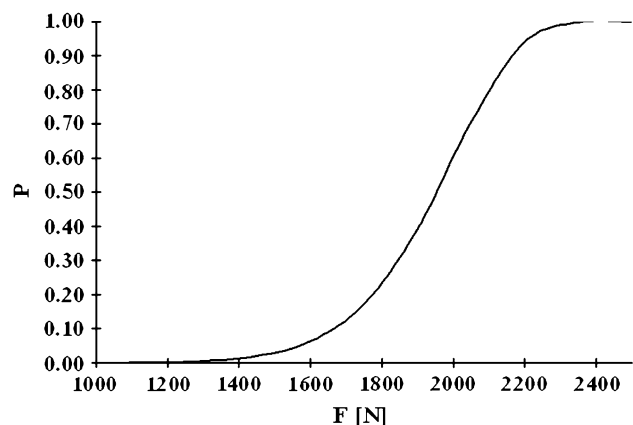


Fig. 7 Probability of failure of the enclosure vs. the applied puncture force

Table 3 Drop-weight impact test results

Drop height, mm	Test number (x = failure, o = pass)										
	1	2	3	4	5	6	7	8	9	10	11
170											x
160								x		o	
150							o		o		
140											
130	x				o						
120		x		o							
110			o								

4. Discussion

The static compressive strength tests showed that the enclosure will surpass the compressive strength required due to the diving criteria. The high compressive strength of the enclosure was expected as alumina has been proven to have very high compressive strength. The large variation in compression results was expected and is likely a result of the variation in the inherent flaw sizes of alumina (Ref 13). Many researchers have reported alumina's cyclic fatigue strength between 86 and 130 ± 10 MPa [Ref 12, 40-42]. These reported fatigue strengths are much higher than the test conditions in the present experiments where the mean and maximum compressive stress applied were 7.78 and 14.94 MPa, respectively. However, since none of the 10 samples failed during 70,000 cycles of loading it is unlikely that the enclosure would fail in service as the mean stress is only 1.33 MPa during diving. Note that during compressive loading of the enclosure most of the load is carried by the side-walls of the box (Fig. 1) and that the stress reported is the nominal stress acting over the whole enclosure. The presence of the epoxy, filling the interior of the enclosure, played an important role in reducing the stresses in the cover of the enclosure. Without epoxy, the cover would deflect in the middle putting a tensile stress in the bottom side of the cover. This can be extremely important as the strength of ceramics is much lower in tension and premature failure of the enclosure will originate from the area under tension.

Puncture tests, which simulate sea lion biting, showed good resistance to failure with the probability of fracture being only 5% at approximately 1500 N. Comparing this to the expected applied force for Steller sea lion's using the African lion as a model; the enclosure will fail at approximately three times the assumed bite force of 440 N. The load causing failure correlates well with what has been observed for alumina under other indentation loading, as a force of 2000 N has been seen as initiating cracking by another research group (Ref 43). During puncture tests, the importance of the epoxy filler is clearly shown. If no epoxy is used to fill the inner cavity of the enclosure, the lid will deform like a simply supported plate under point loading. This creates a tensile stress on the bottom side of the lid and due to the low tensile strength of alumina, failure will occur at low stress levels. The presence of the epoxy filler provides stiffness to the enclosure and prevents excessive bending of the lid. This significantly improves the resistance of the enclosure to puncture or any other localized load.

In the impact tests, alumina specimens showed similar mean failure energy (6.7 J) to what has been reported elsewhere for alumina (Ref 29-31, 44). This failure energy was compared to the readily available adult human skull fracture energies, which lies between 20 and 73 J (Ref 36, 37, 45-48). The stiffness or resistance to deformation of a human infant skull is 12-25 times lower than that of the adult skull (Ref 49-51), which implies lower skull fracture energy for infants. Calculations of the kinetic energy of a pup head free falling onto a rock showed that a fall of approximately 0.3 (the approximate height of a pup), 1, and 3 m (typical cliff height) produces impact energies of 17, 56, and 170 J, respectively. A comparison of these energies to alumina and skull fracture energies shows that both an infant skull (assuming a fracture energy of 20 J from the lower end of the data range) and enclosure are both likely to break at falls >1 m. Falls at the height of the sea lion might or might not affect both skull and alumina enclosure. Uncertainty

arises due to the wide range of reported skull failure energies. Unlike the results from the other service tests and fall distances, there is no comfortable safety margin.

Short falls that are capable of producing skull fracture energies actually seldom cause skull injuries in young humans (Ref 52). The explanation for this is the majority of the impact energy is absorbed by surrounding tissue, the neck, or other body parts. It is likely surrounding tissue would offer the needed margin of safety. Skin and subcutaneous tissue of the human forearm with thickness of 2 mm were found to absorb 30-55% of the total impact energy (Ref 27). Using an impact pendulum and surrogate human pelvis, fall impact experiments have shown that trochanteric soft tissues with thickness ranging from 8 to 45 mm absorbed 8.4 to 81.6 J of energy when exposed to peak force ranging from 4,050 to 11,000 N (Ref 26, 45, 47). Tissues in the human scalp have been shown to be similar to silicon rubber in nature and to be able to absorb 15 J of energy (Ref 53). Assuming that the tissues surrounding an embedded enclosure give similar effects, 3 mm of blubber above the scalp of a sea lion pup (Ref 54) in which the enclosure would likely be implanted, and a skin thickness above the device of 2.5 mm (Ref 55), the tissues surrounding the enclosure could absorb approximately 30% or 5-10 J of the impact energy due to a 0.5 m fall. As skin and blubber thicknesses increase as the animal ages, wild life researchers might consider waiting until the blubber layer in a pup reaches a thickness of 1 cm before implanting the new RF device within it. The 1.3 cm of tissue could absorb the impact energy due to a 0.5 m fall by approximately 10-20 J, and provide a margin of safety. As the animal grows, the device must remain within the blubber layer. More research should be carried out on how and where a device fixates under the skin of a growing animal before the devices are placed under the skin of the young of endangered wild animals.

The effect on the enclosure due to impacting flippers was calculated to be 81, 160, and 250 J for 200, 350, and 1000 kg bulls, respectively. These impact forces would easily fracture the head of a pup and likely also the enclosure, and helps explain why pups are often killed when trampled.

5. Conclusions

In order to design a telemetry device for tracking the whereabouts of growing Steller sea lions, reliability experiments were conducted to assess the resistance of the device enclosure to in-service loading conditions that will be experienced during sub-dermal implantation. Compression, cyclic fatigue, and puncture tests all showed results that passed the set criteria. Cyclic fatigue results showed no enclosure failure after 70,000 cycles for stresses of approximately 15 MPa for with a 90% reliability; compression results show failure of the enclosure at a minimum stress level of 259 MPa for a 5% probability of failure; and puncture forces at failure are at a minimum level of 1568 N for a 5% probability of failure. The response of the enclosure to impact was failure at a mean energy level of 6.7 J. Calculations showed that free falls greater than a distance of 1 m and device impact due to trampling by raging bulls would break both the enclosure and the underlying skulls. To provide a margin of safety against short distance impact, devices should be implanted within an impact absorbing 1 cm thick blubber layer. Although no test animals were available, the conservative

testing and analysis methods were developed to demonstrate reliability of the enclosure over the 20-30-year lifetime of the sea lion. More research should be conducted on how and where the enclosure fixates under the skin of growing animals before implanting the RF device into the young of endangered animals that could suffer head impacts.

Acknowledgments

This research was supported by a grant from the North Pacific Marine Science Foundation to the North Pacific Universities Marine Mammal Research Consortium.

References

1. A.W. Trites and D. Pauly, Estimating Mean Body Masses of Marine Mammals from Maximum Body Lengths, *Can. J. Zool.*, 1998, **76**, p 886–896
2. National Research Council, The Decline of the Steller Sea Lion in Alaskan Waters: Untangling Food Webs and Fishing Nets, National Academy Press, Washington DC, 2003, 204 p
3. B.D. Hori, R.J. Petrell, A.W. Trites, and T. Godbey, Lamination for Subdermal Implant Fixation, *J. Biomed. Mater. Res., Part B*, 2009, **91B**(1), p 17–25
4. A. Batchelor and M. Chandrasekaran, *Service Characteristics of Biomedical Materials and Implants*, World Scientific, River Edge, 2004
5. P. Wilmshurst, Cardiovascular Problems in Divers, *Heart*, 1998, **80**, p 537–538
6. T. Loughlin, J. Sterling, R. Merrick, J. Sease, and A. York, Diving Behavior of Immature Steller Sea Lions (*Eumetopias jubatus*), *Fish. Bull.*, 2003, **101**, p 566–582
7. B. Mate, Northern (Steller) Sea Lion. In: *Mammals in the Seas. Pinniped Species Summaries and Report on Sirenians*, FAO Fisheries Series, Vol. 2, 1979, p 1–4
8. Y. Lee, J. Pan, R. Hathaway, and M. Barkey, *Fatigue Testing and Analysis: Theory and Practice*, Elsevier, Oxford, 2005
9. A. Kaplan, Effect of Loading Cycle Parameters on Fatigue-Crack Growth (Review), *Moscow Aviat. Inst.*, 1978, **14**, p 58–68
10. J. Matthewson and V. Padiyar, Cyclic Fatigue of High Strength Optical Fibers in Bending, *Proceedings of the International Society for Optical Engineering*, Vol. 4215, November 2000 (Boston, MA), 2001, p 53–59
11. Standard Practice for Conducting Amplitude Axial Fatigue Tests of Metallic Materials, e466-07, Book of Standards, Vol. 3.01, ASTM, p 465–469
12. D. Munz and T. Fett, *Ceramics: Mechanical Properties, Failure Behaviour, Materials Selection*, Springer, Berlin, 1999
13. S. Suresh, *Fatigue of Materials*, Cambridge University Press, New York, 1998
14. J. Wachtman, *Mechanical Properties of Ceramics*, Wiley-Interscience, New York, 1996
15. K. Kohyama, E. Hatakeyama, T. Sasaki, H. Dan, T. Azuma, and K. Karita, Effects of Sample Hardness on Human Chewing Force: A Model Study Using Silicone Rubber, *Arch. Oral Biol.*, 2004, **49**, p 805–816
16. S. Wroe, C. McHenry, and J. Thomason, Bite Club: Comparative Bite Force in Big Biting Mammals and the Prediction of Predatory Behaviour in Fossil Taxa, *Proc. R. Soc. B*, 2005, **272**, p 619–625
17. C. Homewood, Cracked Tooth Syndrome—Incidence, Clinical Findings and Treatment, *Aust. Dent. J.*, 1998, **43**(4), p 217–222
18. M. Rosentritt, T. Plein, C. Kolbeck, M. Behr, and G. Handel, In Vitro Fracture Force and Marginal Adaptation of Ceramic Crowns Fixed on Natural and Artificial Teeth, *Int. J. Prosthodont.*, 2000, **13**, p 387–391
19. M. Collantes, Evaluation of the Importance of Using the Head Injury Criterion (HIC) to Estimate the Likelihood of Head Impact Injury as a Result of a Fall onto Playground Surface Materials, US Consumer Product Safety Commission, 1990
20. M.D. Smith, J.D. Burrington, and A.S. Woolf, Injuries in Children in Free Falls: An Analysis of 66 Cases, *J. Trauma*, 1975, **15**, p 987–991
21. R.L. Gentry, Development of Social Behavior Through Play in Steller Sea Lion, *Am. Zool.*, 1974, **14**(1), p 391–403
22. F.E. Sandegren, Courtship Display, Agonistic Behavior and Social Dynamics in Steller Sea Lion (*Eumetopias jubatus*), *Behavior*, 1976, **57**, p 159–167
23. A.J. Winship, A.W. Trites, and D.G. Calkins, Growth in Body Size of the Steller Sea Lion (*Eumetopias jubatus*), *J. Mammal.*, 2001, **82**(2), p 500–519
24. E. Årgen, L. Nordenberg, and T. Mörner, Surgical Implantation of Radiotelemetry Transmitters in European Badgers (*Meles meles*), *J. Zool. Wildlife Med.*, 2000, **31**(1), p 52–55
25. S.J. Thurlow, Impact Tests on Human Occipital Scalp Material, *Br. J. Exp. Pathol.*, 1963, **5**, p 538–545
26. S.N. Robinovitch, T.A. McMahon, and W.C. Hayes, Force Attenuation in Trochanteric Soft Tissues During Impact from a Fall, *J. Orthop. Res.*, 1995, **13**, p 956–962
27. V. Nikolić, J. Hančević, M. Hudec, and B. Banović, Absorption of the Impact Energy in the Palmar Soft Tissues, *Anat. Embryol.*, 1999, **148**, p 215–221
28. “Standard Test Method for Impact Resistance of Flat, Rigid Plastic Specimen by Means of a Striker Impacted by a Falling Weight (Gardner Impact),” D 5420, Book of Standards, Vol. 8:03, ASTM, p 457–463
29. “Standard Test Method for Resistance of Organic Coatings to the Effects of Rapid Deformation (Impact),” D 2794-93(2004), Book of Standards, Vol. 6.01, ASTM, p 378–379
30. E. Dorre and H. Hubner, *Alumina*, Springer, Berlin, 1984
31. S. Maher, J. Lipman, L. Curley, M. Gilchrist, and T. Wright, Mechanical Performance of Ceramic Acetabular Liners Under Impact Conditions, *J. Arthroplasty.*, 2005, **18**, p 936–941
32. D. Sherman and T. Ben-Shushan, Quasi-static Impact Damage in Confined Ceramic Tiles, *Int. J. Impact Eng.*, 1998, **21**, p 245–265
33. V. Madhu, K. Ramanjaneyulu, T. Bhat, and N. Gupta, An Experimental Study of Penetration Resistance of Ceramic Armour Subjected to Projectile Impact, *Int. J. Impact Eng.*, 2005, **32**, p 337–350
34. A. Rajendran and D. Dandekar, Inelastic Response of Alumina, *Int. J. Impact Eng.*, 1995, **17**, p 649–660
35. J. Lopez-Puente, A. Arias, R. Zaera, and C. Navarro, The Effect of the Thickness of the Adhesive Layer on the Ballistic Limit of Ceramic/Metal Armours. An Experimental and Numerical Study, *Int. J. Impact Eng.*, 2005, **32**, p 321–336
36. K. Johnson, T. Fischer, S. Chapman, and B. Wilson, Accidental Head Injuries in Children under 5 Years of Age, *Clin. Radiol.*, 2005, **60**, p 464–468
37. J. Wood, Dynamic Response of Human Cranial Bone, *J. Biomech.*, 1971, **4**, p 1–12
38. C. Farley, J. Glasheen, and T. McMahon, Running Springs: Speed and Animal Size, *J. Exp. Biol.*, 1993, **185**, p 71–86
39. M. Ghadiri and Z. Zhang, Impact Attrition of Particulate Solids. Part 1: A Theoretical Model of Chipping, *Chem. Eng. Sci.*, 2002, **57**, p 3659–3669
40. J. Healy, A. Bushby, Y. Mai, and A. Mukhopadhyay, Cyclic Fatigue of Long and Short Cracks in Alumina, *J. Mater. Sci.*, 1997, **32**, p 741–747
41. S. Lathabai, Y. Mai, and B. Lawn, Cyclic Fatigue Behavior of an Alumina Ceramic with Crack-Resistance Characteristics, *J. Am. Ceram. Soc.*, 1989, **72**, p 1760–1763
42. Q. Zheng, X. Zheng, and F. Wang, On the Expressions of Fatigue Life of Ceramics with Given Survivability, *Eng. Fract. Mech.*, 1996, **53**, p 49–55
43. F. Guiberteau, N. Padture, and B. Lawn, Effect of Grain Size on Hertzian Contact Damage in Alumina, *J. Am. Ceram. Soc.*, 1994, **77**, p 1825–1831
44. X. Huang and M. Tu, Effect of Single Impact Damage on Strength of Alumina and Zirconia-Toughened Alumina, *J. Mater. Sci. Lett.*, 1996, **15**, p 1925–1926
45. P. Verschuere, H. Delye, B. Depreitere, C. Van Lierde, B. Haex, D. Berckmans, I. Verpoest, J. Goffin, J. Vander Sloten, and G. Van der Perre, A New Test Set-Up for Skull Fracture Characterization, *J. Biomech.*, 2007, **40**(15), p 3389–3396
46. E. Gurdjian, J. Webster, and H. Lissner, Studies on Skull Fracture with Particular Reference to Engineering Factors, *Am. J. Surg.*, 1949, **78**(5), p 736–742
47. N. Yoganandan, J. Zhang, and F. Pintar, Force and Acceleration Corridors from Lateral Head Impact, *Traffic Inj. Prev.*, 2004, **5**(4), p 368–373

48. P. Holck, What Can a Baby's Skull Withstand? Testing the Skull's Resistance on an Anatomical Preparation, *Forensic Sci. Int.*, 2005, **151**, p 187–191
49. M. Kleinberger, N. Yoganandan, and S. Kumaresan, Review: Biomechanics of Child Occupant Protection, *Traffic In. Prev.*, 2000, **2**(1), p 63–73
50. O. Mohan, B. Bowman, R. Snyder, and D. Foust, A Biomechanical Analysis of Head Impact Injuries to Children, *J. Biomech. Eng.*, 1979, **101**, p 250–259
51. B. Coats and S. Margulies, Material Properties of Human Infant Skull and Suture at High Rates, *J. Neurotrauma*, 2006, **23**, p 1222–1232
52. T.L. Lyons and R.K. Oates, Falling Out of Bed: A Relatively Benign Occurrence, *Pediatrics*, 1993, **92**, p 125–127
53. S.J. Thurlow, Impact Tests on Human Occipital Scalp Material, *Br. J. Exp. Pathol.*, 1963, **5**, p 538–545
54. R.A.H. Jonker and A.W. Trites, Morphometric Measurements and Body Conditions of Healthy and Starving Steller Sea Lion Pups (*Eumetopias jubatus*), *Aquat. Mamm.*, 2000, **26**, p 151–157
55. K.O. Olawale, R.J. Petrell, D.G. Michelson, and A.W. Trites, The Dielectric Properties of the Cranial Skin of Five Young Captive Steller Sea Lions (*Eumetopias jubatus*), and a Similar Number of Young Domestic Pigs (*Sus scrofa*) and Sheep (*Ovis aries*) Between 0.1 and 10 Ghz, *Physiol. Meas.*, 2005, **26**, p 627–637